Karlsruhe Institute of Technology

Lecture: Accelerator Physics
Winter 2024/25

Magnet Technology

Axel Bernhard

Contents

1 A brief guide to materials

1.1 Ferromagnetic materials

Accelerator magnets are technically implemented in a variety of ways, depending on the application. However, magnets that are purely coil-based are the exception and are only used where fast-pulsed magnetic fields without hysteresis, e.g. in the area of injection and ejection of particles in a ring accelerator. Apart from these exceptions, ferromagnetic materials are widely used as yokes, poles and also as field sources (permanent magnets). The macroscopic magnetic properties of these materials are important for the achievable fields and multipole strengths, but also for the field quality.

The microscopic origin of ferromagnetism lies in the non-vanishing magnetic moments of the electrons in incompletely filled shell levels (more precisely, their unpaired spins), which are significantly present in particular in the $3d$ metals (Fe, Co, Ni) and rare earths ($4f$ metals, Ce-Yb).

A distinction is made between

- hard magnetic materials (permanent magnets): significant macroscopic magnetic moment even in the absence of an external magnetic field
- soft magnetic materials: macroscopic magnetic moment when aligned by an external magnetic field

Permanent magnetism is usually the result of magnetocrystalline anisotropy, i.e. a preferred direction of magnetisation predetermined by the crystal structure, referred to in the literature as the *easy axis*.

It is well known that in the absence of an 'external' magnetic field, the magnetic flux density inside a ferromagnetic material is determined by the magnetisation density

$$\vec{B} = \mu_0 \vec{M}. \tag{1.1}$$

To describe macroscopic magnetisable media in an external field, the magnetic field (the magnetising force) $\vec{H}$ is introduced with

$$\begin{aligned} \vec{B} &= \mu_0(\vec{H} + \vec{M}) \quad = \mu_0(1 + \chi_m)\vec{H} \\ &= \mu\vec{H}, \end{aligned} \tag{1.2}$$

where χ_m is referred to as magnetic susceptibility and μ as magnetic permeability. In general, these two quantities are tensorial (i.e. anisotropic) and non-linear.

The properties of magnetic materials can now be described to a large extent on the basis of their behaviour when subjected to an external magnetic field.

1.1.1 Permanent magnets

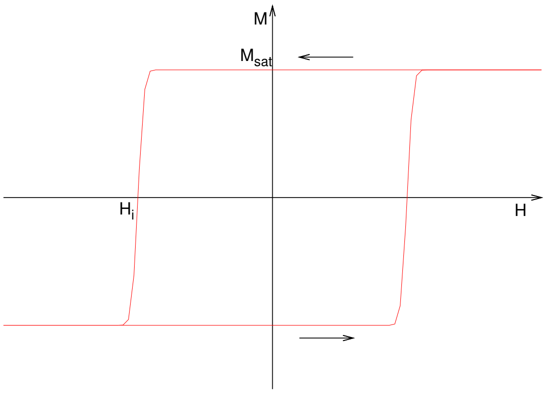

Figure 1: Magnetisation curve of a permanent magnet (schematic)

Hard magnetic materials are characterised by a „broad“ hysteresis in the magnetisation, i.e. by the preservation of the saturation magnetisation M_{sat} even for relatively high opposing ‘external’ magnetic fields.

The magnetic field strength at which the magnetisation flips (more precisely: becomes zero) is called the intrinsic coercivity of the material.

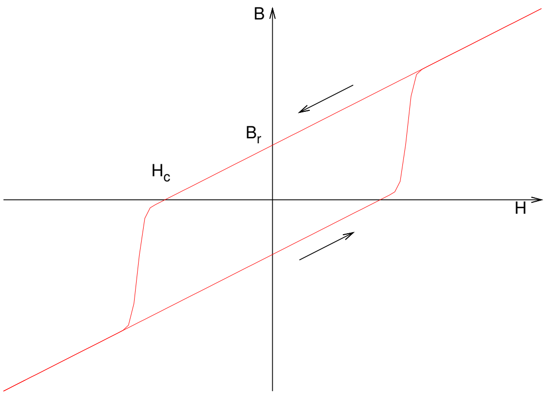

Figure 2: B-H curve of a permanent magnet

Further important parameters are the points of intersection of the magnetic flux density as a function of the magnetic field with the coordinate axes:

- B_r: remanence field, i.e. the remaining flux density at $H = 0$
- H_c: coercive force, coercive force, the magnetic field needed to bring the flux density to zero

The magnetisation of a permanent magnet itself generates a field H inside the magnet, which counteracts the magnetisation. The operating point of a permanent magnet is therefore always in the second quadrant of the B-H curve! Where on this curve the working point lies depends on the geometry of the magnet (more precisely, the ratio of the area perpendicular to the easy axis to the side length parallel to the easy axis) and the external field. In an undulator, a non-vanishing external field is always caused by the neighbouring magnets, which may also have a demagnetising effect.

In the case of an ideal permanent magnet, the entire curve segment in the 2nd quadrant is linear. In the non-ideal case, the second quadrant already shows the non-linear descent to the lower branch of the hysteresis loop. If the operating point enters the non-linear area of the B-H curve, this will lead to non-reversible demagnetisation.

The B-H curve is usually temperature dependent: with increasing temperature both the remanence field and the coercivity usually decrease.

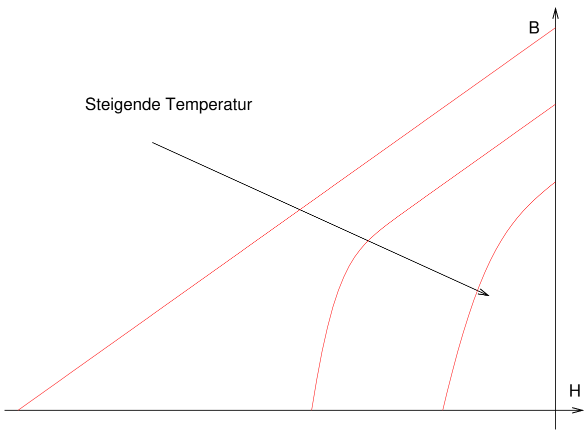

Figure 3: B-H curve of permanent magnets as a function of temperature (schematic)

Permanent magnets are widely used, especially (but not only) in the construction of undulators and wigglers. In the design and operation of insertion devices, the properties of permanent magnets mentioned above must be taken into account and lead to limitations on achievable periods or permissible operating temperatures and radiation levels.

Examples of transition metal/rare earth hard magnetic materials:

Materials

	Remanence field [T]	Coercivity [kA/m]	Rem.
$SmCo_5/Sm_2Co_{17}$	0.85-1.05	600-800	suitable for high temperatures, brittle
$Nd_2Fe_{14}B$	1.1-1.4	750-1000	limited suitability for high temperatures, less brittle

The manufacturing process for hard magnetic semi-finished products from these metallic alloys comprises the following steps:

- alloying (melting under vacuum or inert gas)
- pulverisation to (3-7) µm grain size; the grains are then largely homogeneous with regard to the main direction of magnetisation (*easy axis*)
- pressing in an external magnetic field to align the *easy axis* (unidirectional or isostatic)
- sintering (by heating to sintering temperature)
- mechanical finishing/shaping
- magnetisation in an external field (typically in a solenoid)

1.1.2 Soft magnetic materials

Soft magnetic materials are used for the poles and yokes of accelerator magnets and undulators. In particular, for coil-excited accelerator magnets, it is advantageous to have the smallest possible hysteresis, i.e. small intrinsic coercivities.

In magnet construction, where moderate rates of change of the fields are usually given, the material of choice is pure iron (*low carbon steel*).

Materials

	Remanence field [T]	Coercivity [A/m]	Note
Fe	-	60-80	

In order to minimise eddy currents in the magnetic poles during ramping (important for synchrotrons in which the magnetic field strengths are cyclically ramped from minimum to maximum value and back again), the yokes/poles are often laminated, i.e. constructed from stacked, soft magnetic sheets, known as laminations, that are insulated from each other. These are typically either glued over their entire surface or welded with steel strips.

1.2 Superconductors

Superconductors are used in the construction of high-field accelerator magnets for high-energy storage rings, but also of undulators. As a rule, these are type-II low-temperature superconductors, rarely high-temperature superconductors.

Reminder: Superconductors of the second kind are characterised by the existence of the so-called SHUBNIKOV phase. In this phase, an ‘external magnetic field is not completely displaced from the volume of the superconductor, but flux tubes (vortices) form in which the field is enclosed. This means that superconductors of type II can be operated at significantly higher external fields than those of type I, which is particularly advantageous for use in high-field magnets.

Superconductor

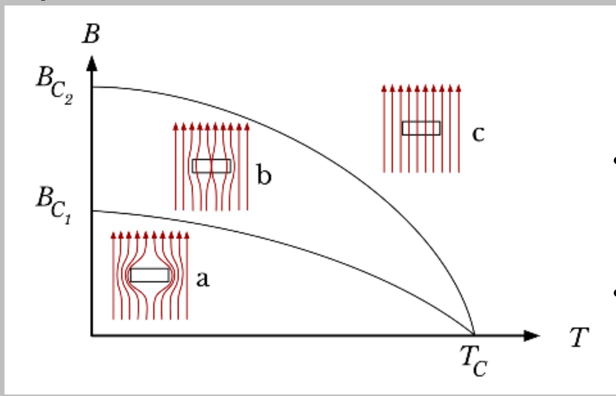

Figure 4: Phase diagram Type-II-Superconductor, Bobroff 2011

- in the high-field accelerator magnet construction typically: type-II low-temperature superconductor
- current R&D: high-temperature superconductor

Technical cryogenic superconductors in magnet construction are typically present as multifilament wires (several tens to hundreds of twisted superconducting filaments embedded in a copper wire). In almost all operational superconducting accelerator magnets today, Nb-Ti alloy is used as the superconducting material.

The use of Nb_3Sn (Type-II low-temperature superconductor) and (at a still early stage of development) of *Rare Earth Barium Cuprate* (REBCO) high-temperature superconductors is the subject of current research and development. Here, tape-shaped technical superconductors are used.

Technical superconductors

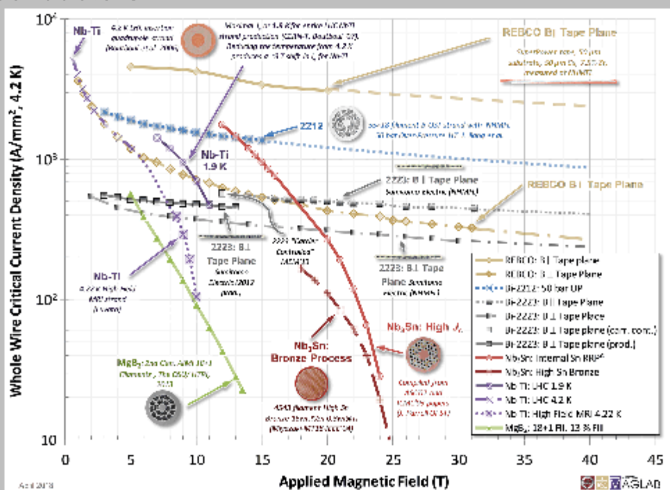

source: *Je_vs_B-041118_1280x929_PAL.Png* 2020

The graph shows the critical current density plotted 'over the external magnetic field at the location of the conductor for various technical superconductors as they are already used in magnet construction today (Nb-Ti at 4.2 K or 1.9 K) or in the further development of accelerator magnets (Nb_3Sn, REBCO).

The current density that can actually be achieved in a specific magnet is given, on the one hand, by the phase boundary shown in the graph and, on the other hand, by the magnetic design, which determines the magnetic flux density that the magnet itself generates at the location of the conductor. This dependency is described by the so-called *load line*. The maximum current density then results from the intersection of the load line with the phase boundary.

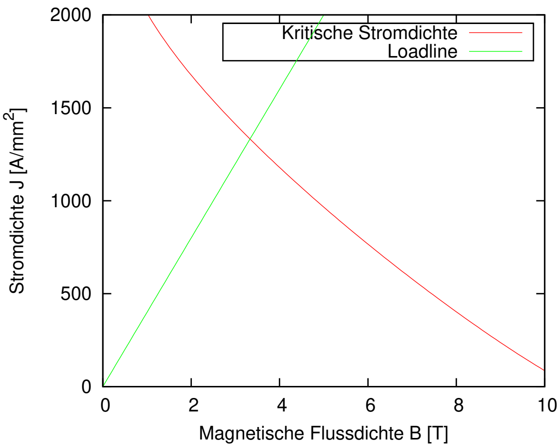

Figure 5: Example: critical current density at $T = 4.2\,\mathrm{K}$ for an Nb-Ti multifilament conductor (EAS F56). The dependence of the external magnetic flux density at the location of the conductor, the *load line*, results from the coil geometry and the yoke material used.

Superconducting magnets are typically operated up to a maximum of 80% of the critical current density on the load line.

References

Bobroff, Frederic Bouquet and Julien (Dec. 2011). *Superconductor Interactions with Magnetic Field*. URL: https://commons.wikimedia.org/wiki/File:Superconductor_interactions_with_magnetic_field.png (visited on 01/07/2021).

Je_vs_B-041118_1280x929_PAL.Png (2020). URL: https://fs.magnet.fsu.edu/~lee/plot/Je_vs_B-041118_1280x929_PAL.png (visited on 01/09/2020).

2 Undulator technology

Magnetic technologies for insertion devices

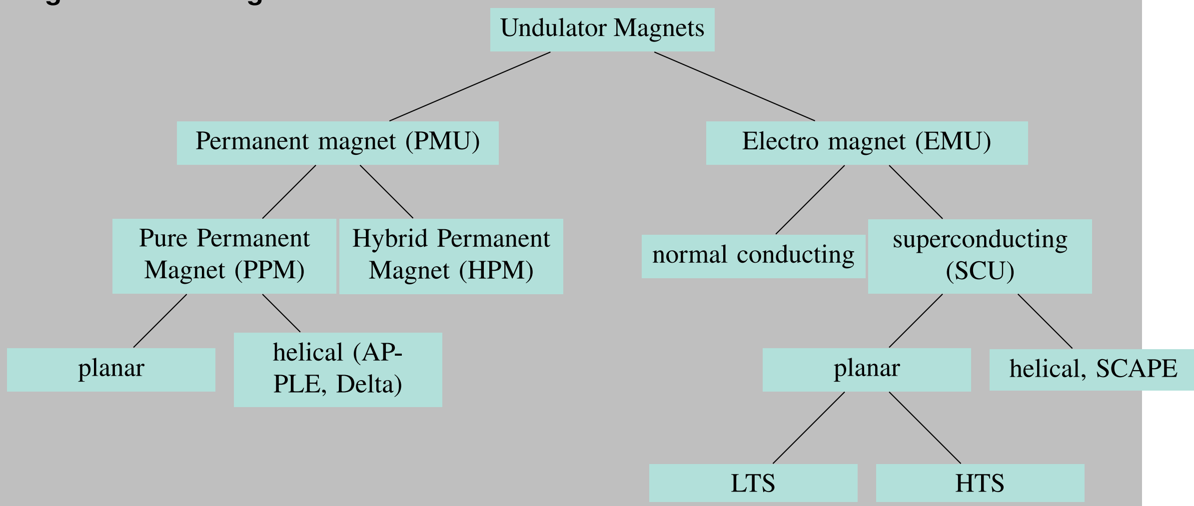

2.1 Permanent magnet undulators

2.1.1 Pure Permanent Magnets (PPM)

Pure Permanent Magnet (PPM)

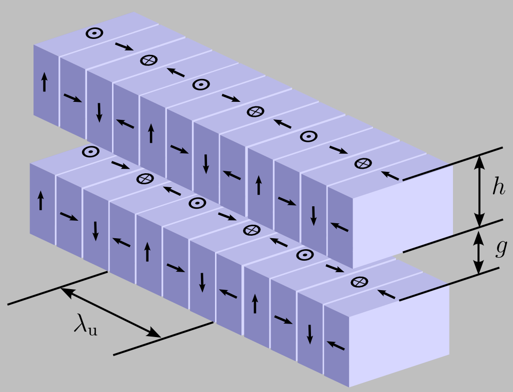

Design principle (K. Halbach NIM 187 (1981))

- permanent magnet blocks
- rotation of easy axis in M steps per period (minimum 4)
- *amplitude determined by B_r, g and λ_u (H_c)*
- tuning by variation of g

Principle: Rotation of the *easy axis* over M homogeneously magnetised segments per period (4 in the example).

For pure permanent magnets, an analytical description of the magnetic field in the gap can be found (for the 2D problem in the y-z plane). It applies

$$
\begin{aligned}
B_y &= -2B_r \sum_{i=0}^{\infty} \cos\left(\frac{2n\pi z}{\lambda_\mathrm{u}}\right) \cosh\left(\frac{2n\pi y}{\lambda_\mathrm{u}}\right) \frac{\sin(n\pi\epsilon/M)}{n\pi/M} \mathrm{e}^{-n\pi g/\lambda_\mathrm{u}} (1 - \mathrm{e}^{-2n\pi h/\lambda_\mathrm{u}}) \\
B_z &= 2B_r \sum_{i=0}^{\infty} \sin\left(\frac{2n\pi z}{\lambda_\mathrm{u}}\right) \sinh\left(\frac{2n\pi y}{\lambda_\mathrm{u}}\right) \frac{\sin(n\pi\epsilon/M)}{n\pi/M} \mathrm{e}^{-n\pi g/\lambda_\mathrm{u}} (1 - \mathrm{e}^{-2n\pi h/\lambda_\mathrm{u}})
\end{aligned}
\tag{2.1}
$$

with $n = 1 + iM$ and the packing density of the permanent magnets ϵ.

Remark. With increasing segmentation M, the field on the axis approaches a pure cosine field.

Remark. When the geometric quantities λ_u, g and h are scaled together, the field amplitude remains constant. In contrast to this, the current density must be scaled in an electromagnet!

A practical rule of thumb for four blocks per period and $h = \lambda_\mathrm{u}/2$ is:

$$B_{y0} = 1.72 B_r \mathrm{e}^{-\pi g/\lambda_\mathrm{u}} \tag{2.2}$$

The importance of the ratio of gap to period length for the scaling of the field amplitude (and thus of the undulator parameter) can be clearly seen here once again.

2.1.2 Hybrid undulators

Hybrid permanent magnet

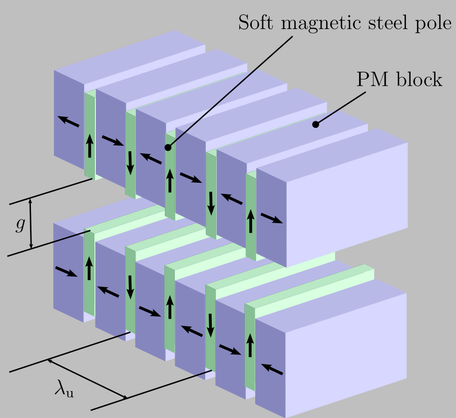

Design principle (K. Halbach (1983))

- soft magnetic poles magnetized by permanent magnet blocks
- non-linear material, numeric field calculation required (FEM)
- practical scaling law

$$B = a \exp\left[b\left(\frac{g}{\lambda_\mathrm{u}}\right) + c\left(\frac{g}{\lambda_\mathrm{u}}\right)^2\right]$$

a, b, c depending on material choice

Halbach 1983

The field calculation for this case must be carried out numerically (typically using the finite element method) because of the non-linearity of the magnetisation curve of the soft magnetic material.

Empirical formulas have been developed for various material combinations on the basis of such calculations, for example for CoSm-based undulators:

$$B_{y0} = 3.33\,\mathrm{T}\exp\left(-5.47\frac{g}{\lambda_\mathrm{u}} - 1.8\frac{g^2}{\lambda_\mathrm{u}^2}\right) \tag{2.3}$$

and for NdFeB

$$B_{y0} = 3.44\,\mathrm{T}\exp\left(-5,08\frac{g}{\lambda_\mathrm{u}} - 1.54\frac{g^2}{\lambda_\mathrm{u}^2}\right) \tag{2.4}$$

Comparison of PPM and HPM

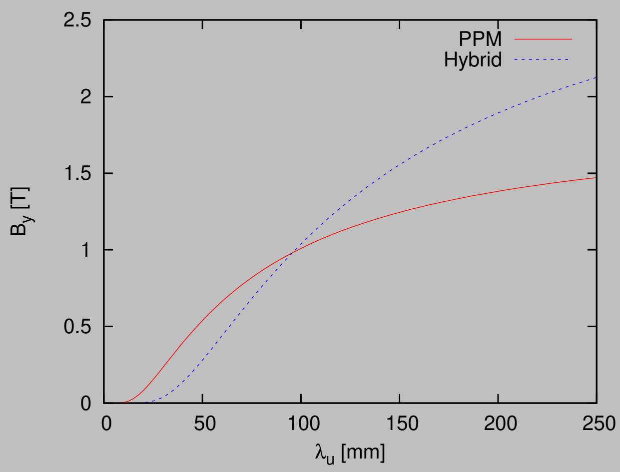

Figure 6: Comparison of the achievable field amplitudes with pure permanent magnets (PPM) and hybrid undulators assuming a remanent field of 1.1 T (SmCo) and a gap of 20 mm.

2.1.3 Excursus: PMU variants

We have seen that the field amplitude that can be achieved for a given period length and magnet geometry in permanent magnet undulators results, on the one hand, from the magnetic properties of the hard and soft magnetic materials used and, on the other hand, from the gap height. The field amplitude and thus the undulator parameter is adjusted by varying the gap height.

The minimum gap and thus the maximum achievable field amplitude, in turn, result from the conditions of the accelerator: necessary beam-stay-clear, beam tube geometry.

Now there is a tendency to use ever more compact accelerators with ever lower particle energies for the generation of synchrotron and FEL radiation, which requires undulators with ever shorter periods. In order to nevertheless achieve sufficiently high field amplitudes (the goal is always $1 < K < 2$) is always the goal, two strategies are being pursued in the field of permanent magnet undulators, in addition to material optimisation: in-vacuum undulators and cooled permanent magnets.

Variants: In-Vacuum Undulators (IVU)

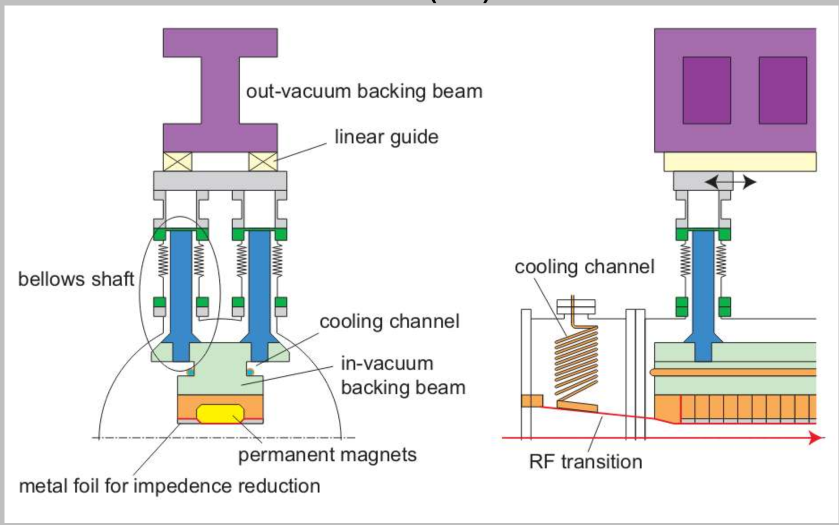

Quelle: Tanaka et al. 2005

Variants: Cooled Permanent Magnets (CPMU)

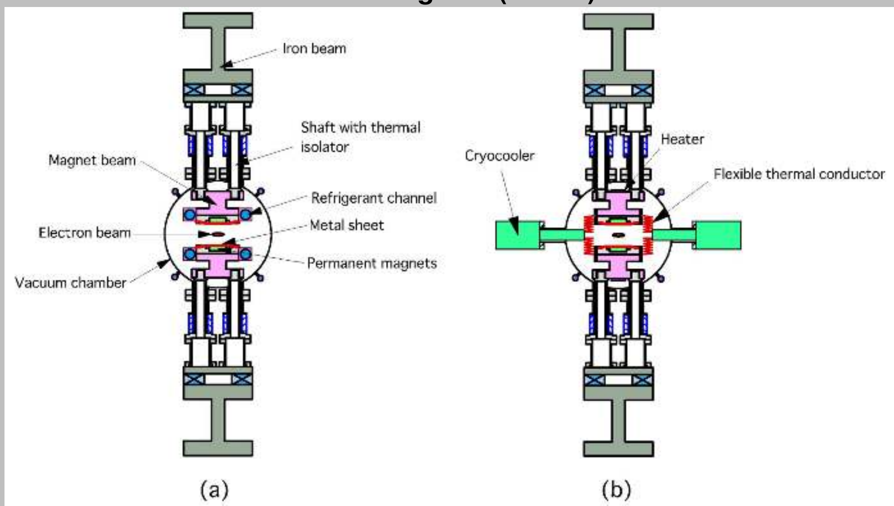

Quelle: Hara et al. 2004

One variant of undulators that has only been mentioned in passing so far should not go unmentioned here because of its importance: undulators for adjustable polarisation of the radiation, i.e. in general for freely selectable elliptical polarisation.

Polarisation control in general is achieved by combining two undulators with orthogonal polarizations (either right-/left-circular or horizontal/vertical planar) with freely adjustable phase between the two.

A common scheme for this is the APPLE scheme:

Permanent magnet variable polarisation (helical) designs

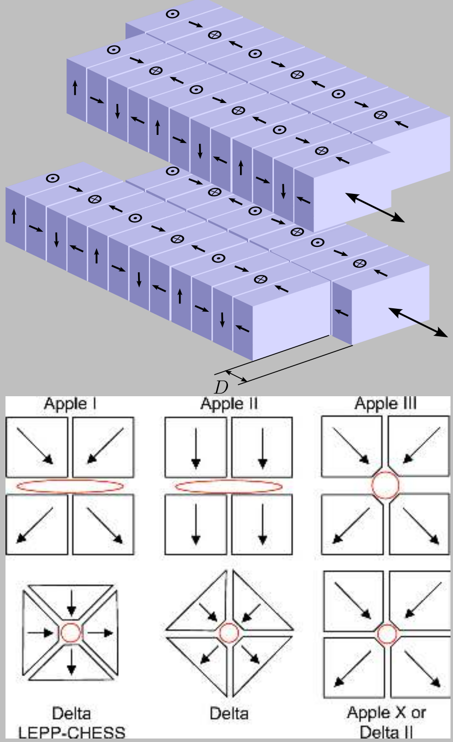

Calvi et al. 2017

Design principles

- 4 magnet arrays for 2 orthogonal field components
- always fixed phase shift of $\frac{\pi}{2}$ between B_x and B_y
- amplitude ratio varies by longitudinal shifting of arrays
- design variations, particularly for round beams
- Scaling law as for planar PMUs, a, b, c additionally depend on the helical undulator design type

2.2 Electromagnetic undulators

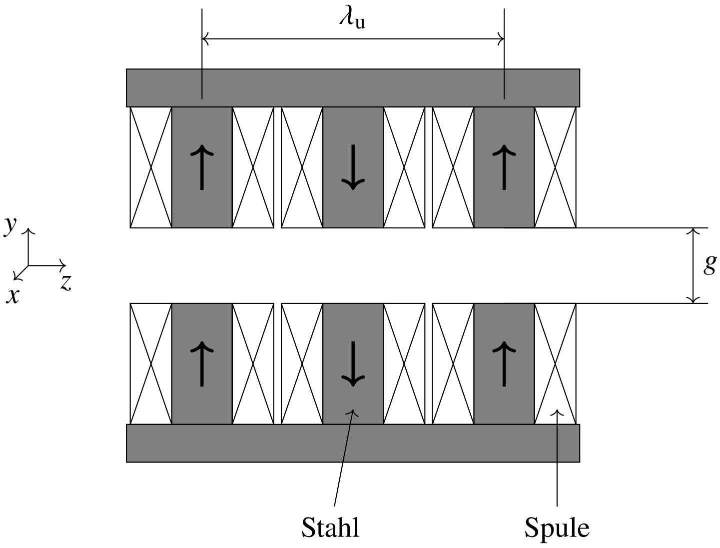

Figure 7: Schematic of an electromagnetic insertion device

Analytical solutions for the field of electromagnetic undulators can be found (using Biot-Savart) if the soft magnetic material is ignored. For the correct consideration of this material, a numerical calculation is also necessary.

For comparison with permanent magnets, let us consider the approximation by electromagnetic dipoles of length $\frac{\lambda u}{2}$. Their field is given by

$$B = \frac{2\mu_0 NI}{g} \tag{2.5}$$

where N is the number of windings and I is the current flowing in them. To characterise the electromagnet, one typically specifies NI in the unit ampere-turns.

(This approximation is only valid for large periods. With decreasing period length, the contribution of the neighbouring dipoles to the field in the half-period under consideration is no longer negligible).

This yields an undulator parameter of

$$K_\mathrm{u} = 2.35 \cdot 10^{-4} NI \frac{\lambda_\mathrm{u}}{g} \tag{2.6}$$

Consequently, several thousand ampere-turns are usually required to achieve an undulator parameter of the order of 1. This number must increase when the period length is shortened. At the same time, however, the space available for the windings decreases, i.e. the current density must be increased.

This is possible if superconductors are used to create the electromagnet. Superconductivity is used both for long-period insertion devices to generate extremely high fields ((3-7) T), and to create particularly short periods.

Electromagnets: Planar SCUs and SCWs

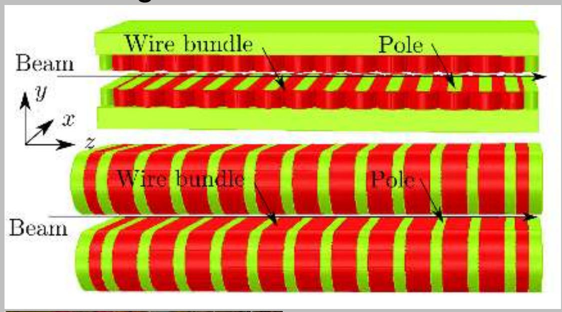

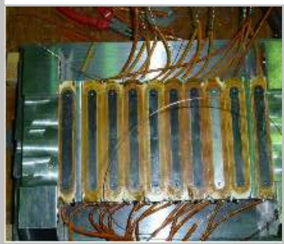

Mezentsev et al. 2016

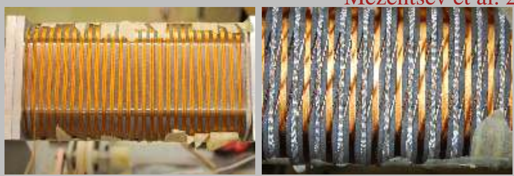

Undulator short model ‘Undine’, built in-house

Richter 2023

HTS vertical racetrack demonstrator coil (1 period)

Aiming at very high fields or short periods
Approximating with dipole field, K_u scales like

$$K_\mathrm{u} = 2.35 \times 10^{-4} N I \frac{\lambda_\mathrm{u}}{g} \tag{2.7}$$

$\Rightarrow$ generally high current densities are required
$\Rightarrow$ SCUs are the mainly relevant EMUs

State of the art

- low temperature SC, Nb-Ti
- horizontal racetrack
  - simple coil procuction (good)
  - many splices (not so good, but manageable)
- vertical racetrack
  - single wire
  - enabling very short periods

On the horizon

- high temperature SC, ReBCO tape
- unprecedentedly high current densities and field amplitudes

SC helical and variable polarisation

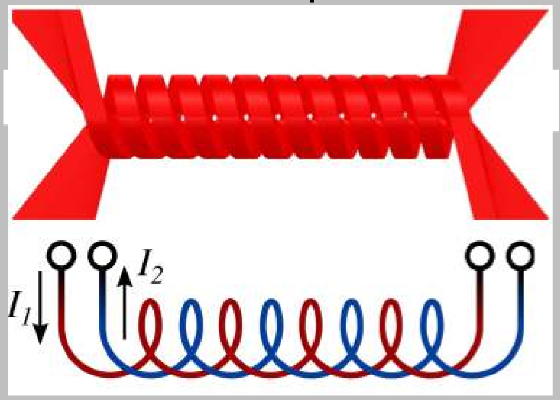

Bifilar helix

- bifilar helical coil around beam pipe
- fixed helicity (not changed upon current inversion)
- extremely resource efficient
- demonstrated for LTS and HTS

Richter 2023

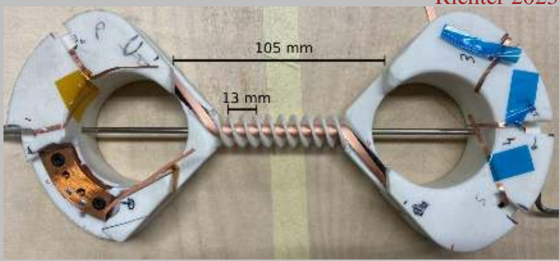

SCAPE

- SC arbitrary polarizing emitter
- full polarization control through two independently powered coil pairs

Richter 2023

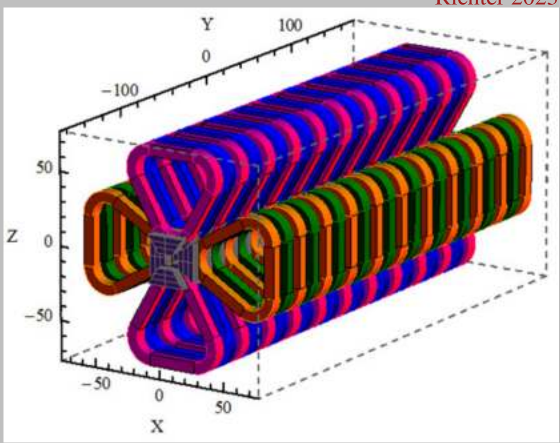

Ivanyushenkov et al. 2017

In a 2D approximation, an analytical expression can be given for the field of such a conductor arrangement (again neglecting the soft magnetic poles):

$$
\begin{aligned}
B_y &= \sum_{m \,\text{odd}} B_m \sin(m k_\mathrm{u} z) \cosh(m k_\mathrm{u} y) \\
B_z &= \sum_{m \,\text{ungerade}} B_m \cos(m k_\mathrm{u} z) \sinh(m k_\mathrm{u} y)
\end{aligned} \tag{2.8}
$$

whereby the following applies as a good approximation:

$$
B_m = \frac{16\mu_0 N I}{\pi \lambda_\mathrm{u}} \frac{\sin(m\pi/4)}{m \sinh(m k_\mathrm{u} g/2)} \tag{2.9}
$$

In typical short-period ($\lambda_\mathrm{u} = (10-20)$ mm) superconducting undulators, currents of (10-20) kA − turns and more can be achieved in the groove.

2.3 Transparency and field termination

The undulator has a finite length $L_\mathrm{u} = N_\mathrm{u}\lambda_\mathrm{u}$, so its field is not strictly periodic.

As an *inserting device*, the undulator field should not affect the beam dynamics as a whole. This means

$$
x(-L_\mathrm{u}/2) = x(L_\mathrm{u}/2) \quad \text{and} \quad \frac{\mathrm{d}x}{\mathrm{d}z}(-L_\mathrm{u}/2) = \frac{\mathrm{d}x}{\mathrm{d}z}(L_\mathrm{u}/2) \tag{2.10}
$$

This is equivalent to

$$
I_1 := \int_{-L_\mathrm{u}/2}^{L_\mathrm{u}/2} B_y(z)\mathrm{d}z = 0 \quad \text{and} \quad I_2 := \int_{-L_\mathrm{u}/2}^{L_\mathrm{u}/2} \mathrm{d}z \int_{-L_\mathrm{u}/2}^{z} B_y(z`)\mathrm{d}z' = 0, \tag{2.11}
$$

because the total deflection and the beam displacement can be directly assigned to the first and second field integrals:

$$
\alpha = \frac{e}{\gamma m c} I_1 \qquad x = \frac{e}{\gamma m c} I_2. \tag{2.12}
$$

In practice, a field that is symmetric or antisymmetric about the centre of the insertion device is usually chosen, and the conditions can be fulfilled with

$$
\begin{aligned}
& B_y(z) = -B_y(-z) \quad \text{and} \quad I_2 = 0 \\
\text{or} \quad & B_y(z) = B_y(-z) \quad \text{and} \quad I_1 = 0.
\end{aligned} \tag{2.13}
$$

This is achieved in both cases when the amplitudes of the last three half-cycles assume the values $\frac{1}{4} : \frac{3}{4} : 1$ in relation to the nominal field amplitude B_{y0}.

The technical solution for achieving these amplitude ratios naturally varies depending on the type of undulator (PPM, hybrid or electromagnet). In symmetrical PPMs, for example, it is possible to terminate with half a magnet block. In the case of the electromagnet, this is possible in the first approximation with half the number of Ampère windings.

In fact, however, a good end-field design that effectively minimises the field integrals for all operating conditions (i.e. gaps or current settings) is an art that can never be perfectly mastered because of the non-linearities that come into play. Therefore, insertion devices are usually additionally equipped with active correction coils for integral correction.

2.4 Magnetic forces and mechanical requirements

A problem that should not be underestimated is the mechanical structure of insertion devices, especially in view of the fact that — in permanent magnet undulators — field properties are varied by means of mechanical movements (this applies to the field amplitude as a function of the gap width, but in helical undulators also to the helicity of the field as a function of the longitudinal displacement of two planar magnet arrangements relative to each other).

To estimate the magnetic forces at work, we consider the change in the stored field energy for an infinitesimal change in the gap width.

The energy density in the gap is

$$\frac{\mathrm{d}W_m}{\mathrm{d}V} = \frac{B^2}{2\mu_0} \tag{2.14}$$

The force corresponds to the work performed per unit of displacement,

$$F = \frac{\mathrm{d}W_m}{\mathrm{d}y} = \int\int \frac{\mathrm{d}W_m}{\mathrm{d}V}\mathrm{d}x\mathrm{d}z = \int\int \frac{B^2}{2\mu_0}\mathrm{d}x\mathrm{d}z \tag{2.15}$$

Assuming a purely sinusoidal dependence in the z direction and constancy in the x direction over a width b (and zero outside), this can be integrated to give

$$F = \frac{B_{y0}^2 L_\mathrm{u} b}{4\mu_0} \tag{2.16}$$

For a realistic PPM undulator with $B_{y0} = 0.54\,\mathrm{T}$ at $\lambda_\mathrm{u} = 50\,\mathrm{mm}$ and with $b = 60\,\mathrm{mm}$ the force between the undulator halves is 3500 N per metre of undulator length.

2.5 Field Errors and their Correction

In addition to the requirements for the field integrals mentioned above, which concern the transparency of the insertion device, the functional principle of the undulators places additional requirements on the local field accuracy.

This is most easily understood using the interference approach. A phase-correct addition of the field amplitudes is only obtained if the electron is in phase with the previously emitted radiation field at every point in the path where it radiates in the forward direction.

The points on the path at which radiation is emitted in the forward direction, z_i (ignoring the finite opening angle), are the points for which

$$x'(z_i) = 0,$$

i.e. the extreme points of the transverse motion, which coincide with the field extrema for field errors that are not too large.

Every error in the field amplitude results in a lengthening of the path travelled by the electron and thus (due to the constant instantaneous velocity) in an error in the phase of the electron with respect to the radiation field.

The ideal phase advance per period is exactly one fundamental wavelength of the undulator radiation (this is the basis for constructive interference).

The difference between the real and ideal phase advance results from the difference in the running times of the photon and electron to

$$\Delta\Phi(z_i) = \frac{2\pi}{\lambda_\mathrm{u}} \frac{2\left(\frac{e}{m_e c}\right)^2 \int_{-\infty}^{z_i} I^2(z`)dz' - K_\mathrm{u}^2 z_i}{2 + K_\mathrm{u}^2} \tag{2.17}$$

with

$$I(z`) = \int_{-\infty}^{z'} B_y(z`')dz`' \tag{2.18}$$

The integration from $-\infty$ means that not only phase differences ‘over one period’ are taken into account, but also a ‘transversal drift accumulated over all periods’.

It can be shown that the variance of the phase over the entire undulator (the so-called rms phase error) correlates with the intensity of the odd harmonics and is thus a good measure of the quality of an undulator.

$$\sigma_\Phi^2 = \frac{\sum_i^{N_p} \Delta\Phi^2(z_i)}{N_p - 1}. \tag{2.19}$$

Here $N_p = 2N_\mathrm{u}$ is the number of poles.

With this phase variance, the ratio of the actual to the ideal radiation intensity on the beam axis for the odd harmonics can be estimated as follows

$$R = \frac{(1 - \mathrm{e}^{-\sigma_\Phi^2})N_p + \mathrm{e}^{-\sigma_\Phi^2} N_p^2}{N_p^2}. \tag{2.20}$$

To maximise the brilliance of the radiation produced, an essential design goal for undulators is to minimise the phase error and, for the reasons given earlier, to minimise the field integrals.

Different strategies are used for permanent magnet and electromagnet undulators

Permanent magnets Sources of error:

- mechanical tolerances of magnet blocks
- magnetisation, magnetisation direction distribution in the individual magnet blocks
- mechanical tolerance of the overall structure (support structure)

To minimise the influence of the individual properties of the magnet block, a two-stage strategy is usually applied:

- Block sorting:

  combinatorial minimisation of phase and trajectory errors. Typically, *simulated annealing* or genetic algorithms are used.

- *Shimming:*

  Application of magnetic shims on the surface of the magnets to compensate for amplitude errors. For example, a shim on a vertical block causes a local increase in the field amplitude. A shim on a horizontal block reduces the field amplitude of both adjacent poles. The transverse position of the shim can also be used to correct multipole errors of both field components.

Electromagnets Sources of error:

- mechanical tolerances of the coil body and windings
- turns faults, earth faults

Here we mean unwanted conductive connections with resistances significantly greater than the resistance of the winding. In the case of superconducting undulators, this is the case for practically every normal-conducting winding or ground fault.

As with permanent magnets, maintaining narrow mechanical tolerances is a necessary condition for small phase and trajectory errors. The problem of block sorting does not arise.

Strategies for fine correction:

- Active shimming using extra current-carrying additional coils

References

Calvi, M. et al. (May 1, 2017). "Transverse Gradient in Apple-type Undulators". In: *Journal of Synchrotron Radiation* 24.3, pp. 600–608. ISSN: 1600-5775. DOI: 10.1107/S1600577517004726.

Halbach, K. (Feb. 1, 1983). "PERMANENT MAGNET UNDULATORS". In: *Le Journal de Physique Colloques* 44.C1, pp. C1–216. ISSN: 0449-1947, 2777-3418. DOI: 10.1051/jphyscol:1983120.

Hara, Toru et al. (May 18, 2004). "Cryogenic Permanent Magnet Undulators". In: *Physical Review Special Topics - Accelerators and Beams* 7.5, p. 050702. DOI: 10.1103/PhysRevSTAB.7.050702.

Ivanyushenkov, Y et al. (2017). "Conceptual Design of a Novel SCAPE Undulator". In: *Proc. of International Particle Accelerator Conference (IPAC'17), Copenhagen, Denmark, 2017*.

Mezentsev, N.A. et al. (2016). *ANKA CLIC Superconducting Multipole Wiggler*. Technical Report 1868879. CERN.

Richter, Sebastian C. (2023). "High-Temperature Superconductor Application to Undulators for Compact Free-Electron Lasers – Anwendung von Hochtemperatursupraleitern auf Undulatoren für kompakte Freie-Elektronen-Laser". PhD thesis. Karlsruhe: Karlsruhe Institute of Technology (KIT). DOI: 10.5445/IR/1000159594.

Tanaka, T et al. (2005). "In-Vacuum Undulators". In: *Proceedings of FEL2005, Stanford, California, USA*.